Evaluation of the Vaisala CL31 ceilometer as a tool for boundary layer characterization within carbon cycle studies

University of Iowa authors:

      Jameson Schoenfelder, Morgan Brown, Alicia Pettibone, and Charles Stanier*
      contact: charles-stanier@uiowa.edu

Abstract

During the period June 18 to July 18, 2008, a Vaisala CL31 ceilometer was operated at the Southern Great Plains (SGP) ARM site in Oklahoma. Then the same instrument was shipped to Iowa and operated at the WBI (West Branch Iowa) tall tower CO2 characterization site. The operation period at WBI was from July 25, 2008 to Aug 26, 2008. The backscatter product from the CL31 was compared qualitatively to three operational measurements at SGP – the previous generation Vaisala CT25K ceilometer, the Micropulse LIDAR, and the four per day rawinsondes. Boundary layer heights were determined manually from inflection points in potential temperature and relative humidity in the rawinsonde data. These were compared to software-determined mixed layer heights from the CL31 using two approaches: Vaisala's MLH software package version 3.0 (a MATLAB executable with extensive graphical user interphase) and a simple boundary layer detection program that finds the point where relative backscatter decays quickest as a function of height.

Qualitative agreement between the three remote sounding instruments was excellent. The spatial and temporal resolution of the CL31 was superior to that of the CT25K, and the signal to noise ratio appears to stay stronger to higher altitudes with the CL31 (compared to the CT25K). At altitudes less than 100 m, the CT25K and CL31 are qualitatively different, with the CT25K usually having a backscatter peak highest at around 80 m, and the CL31 product smoothly increasing up to the a maximum at the surface.

Both algorithms performed well for matching rawinsonde-derived PBL features between 0.5 and 2 km. Ceilometer-derived boundary layer heights were within 15% of the sonde-derived heights in about 60% of the examined cases. For matching sonde features less than 0.5 km (these were not typically mixed layer heights, but rather the height of stable atmospheric boundary layers) only the Vaisala algorithm was used. In this height range, the Vaisala algorithm tended to cluster the height around a smaller range (120-220 m) than determined by the sondes (40-350 m). Therefore, relative error in the boundary layer height is high. Although there was high correlation between rawinsonde-derived PBL features and ceilometer-based features, the multilayer structure of the atmosphere (corresponding to 2-4 different layers in any given launch) will make interpretation of CL31 data alone difficult.

At West Branch, Iowa, the comparison was made between the CL31 product time series (backscatter curtain plots and mixed layer height) and the CO_2 concentrations measured at the three tower elevations of 31, 99 and 379 meters above ground. The time when the mixed layer height grows to these tower heights is clearly observed in the CO_2 record during the growing season. The time of growth to 379 m is tightly correlated with the CL31 mixed layer height.

The time of growth to 99 m is not well correlated with the CL31 mixed layer height, although modification of the processing algorithm for the CL31 could probably be done to improve this agreement.

With respect to carbon cycle studies, there does seem to be a potential to constrain both nocturnal and daytime boundary layer heights at individual sites using ceilometers.   For this to be done operationally, substantial work would be needed (possibly on a site-by-site basis) to fine tune the software so that the appropriate boundary layer features of interest could be identified, especially during periods with multiple layers.

1.0 Introduction and Objectives

During the period June 18 to July 18, 2008, a Vaisala CL31 ceilometer was loaned by Vaisala and operated at the Southern Great Plains (SGP) ARM site in Oklahoma. Then the same instrument was shipped to Iowa and operated at the WBI (West Branch Iowa) tall tower CO2 characterization site. The operation period at WBI was from July 25, 2008 to Aug 26, 2008.

Figure 1. CL31 at ARM-SGP site in Oklahoma. Photo by Victor Morris, PNNL.

The goals of this instrument trial and the subsequent data analysis were as follows:

1. At the SGP site
   - Compare the older CT25K ceilometers and the newer CL31 ceilometer in side-by-side operation at the SGP site
   - Compare boundary layer heights as measured by CL31 aerosol profile, and by MPL lidar backscatter profile
   - Compare boundary layer heights as measured by balloon sounding to those measured by CL31 backscatter profile
2. At the WBI site
   - Compare CL31 BL height to BL evolution as measured by met stations and CO2 readings on the tall tower.
3. Compare various BL heights as measured in the field with WRF coarse (60 km) resolution BL heights used in Carmichael ARCTAS forecasts. Also include operational met fields: NAM, RUC, GFS, ECMWF if available.

This document represents completion of tasks 1 and 2.

This document is structured as follows: section 2 is an experimental section that describes the sites, instruments, and data processing; section 3 discusses the results of the intercomparison at SGP; section 4 includes the WBI results.

Section 2. Experimental and Site Information

2.1 Site Information

The DOE Southern Great Plains (SGP) Site. The SGP site, based near Ponca City, OK, has been in operation since 1993. The Central Facility, which is location of most of the instruments in this analysis, is located at 36° 37' N and 97° 30' W. Further information about SGP about the site, its instruments, and operation can be gathered from www.arm.gov/sites/sgp.stm.

West Branch Iowa (WBI) Site. The NOAA tall tower CO_2 system at WBI is located at the KWKB television transmitter (41° 43' 29.2'' N 91° 21' 10.2'' W). A map image of the tower location is shown below.

KWKB television transmitter, location of new NOAA CO2 "Tall Tower"
41.7248 N   91.3528 W   elev 242 m (NOAA website)
Local Partner to NOAA: Stanier Research Group

Rawinsonde / weather balloon launch site
41.6992 N 91.3453 W   elev 226 m (Google Earth)
2.82 km from tower
Bay Run Farm, owners Larry and Peggy Bailey
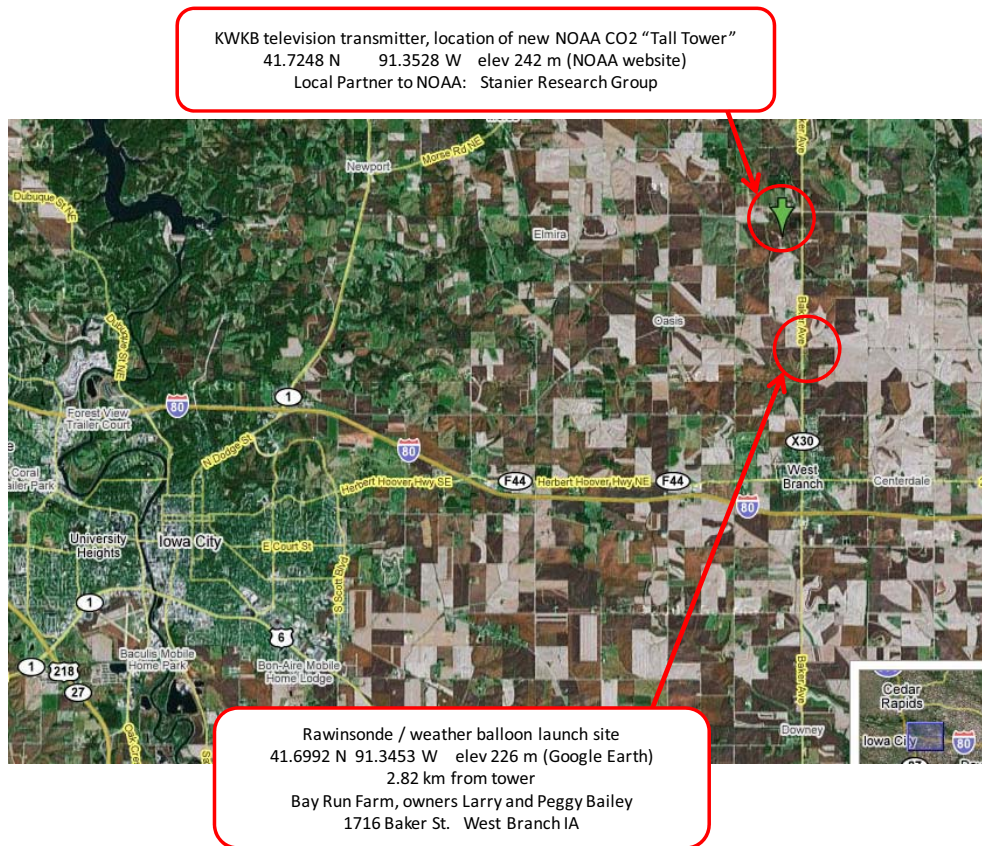1716 Baker St.   West Branch IA

Figure 2. Map showing location of WBI in relation to Iowa City, IA and West Branch, IA

Table 1. Site description and instrument list

	SGP Site	WBI Site
Location	Near Ponca City, OK	West Branch, IA
Lat/Lon	36°37' N 97°30' W	41° 43' 29.2'' N 91° 21' 10.2'' W
Altitude	320 m	
Instruments (* indicates used in this work. For SGP, only instruments used are listed; † indicates for special campaign)	CL31 ceilometer† CT25k ceilometers Weather balloons MPL LIDAR	CL31 ceilometer*† Elastic LIDAR† Continuous CO2 Continuous CO NASA DIAL CO2 LIDAR† Sondes*† Particle number size distribution (ground level) † Tower meteorology
First operation	1993	July 2007

2.2   Instrument Information

Vaisala Ceilometers. Ceilometers measure the vertically resolved backscatter profile using a pulsed laser. Most of the backscatter detected comes from the laser interacting with aerosol and cloud particles in the atmosphere. This backscatter profile allows determination of the boundary layer height (BLH) in the atmosphere. Two instruments are compared in this work. The CT25k ceilometer, and the newer CL31 ceilometer.

Figure 1 shows the CL31 at SGP. Figure 3 shows the CT25k at SGP. Figure 4 shows the CL31 at WBI.

Figure 3. CT25k at SGP. Image source www.arm.gov

Figure 4. CL31 mounted at WBI. Photos by J. Schoenfelder.

SGP Balloon-borne soundings. Rawinsondes were launched about four times a day at ARM during this field campaign. The rawinsonde data of interest when trying to calculate the BLH is the dry bulb temperature, dew point temperature, and potential temperature.

Figure 5. Weather balloon

Figure 6. MPL LIDAR

SGP Micropulse LIDAR. The Micro Pulse Lidar (MPL) also operates by monitoring the return of a laser pulse off of clouds, aerosols, and hydrometeors. In this work the cross polarized return signal is used with a range and overlap correction done at the University of Iowa based on an overlap function provided by Rich Coulter.

Some instrument parameters and data processing parameters can be found in Table 2.

Table 2. Vertical Sounding Instrumentation Details

Rawinsonde at SGP	
Operational period	4/30/1994 – present (4/1/2001 to present with same data level used in this work)
Data source	www.arm.gov
File type	sgpsondewnpnC1.b1 (cdf) files
Data processing	Read into MATLAB using netcdf read.
Average coordinates	36.5637°N -97.2908°E

CL31 at SGP	
Operational period	6/18/2008 to 7/18/2008
Data source / file type	.dat files retrieved from PC connected to ceilometer
Raw data attributes	10 m vertical resolution 15 sec between scans Backscatter recorded in units of $(srad*km*10^5)^{-1}$
Data processing	Converted to text files using CL-view program and imported into MATLAB. A 240 m vertical, 1800 sec time averaging filter used before plotting. Boundary layers determined by two computer programs. The Iowa BL detection method fits a backscatter profile with a fifth order polynomial based on Kovalev and Eichinger (2004). The BL is then defined as the steepest slope (inflection point) for the polynomial. Vaisala's BL heights were found using the Vaisala MLH control application (version 3.0).
For more info	http://www.vaisala.com/weather/products/weatherinstruments/ceilometers/cl31

CL31 at WBI	
Operational period	7/25/2008 to 8/26/2008 Data processed identically to SGP (see above).

CT25k at SGP	
Operational period	9/20/1999 to present
Data source	www.arm.gov
File type	Sgpvceil25kC1.b1 (cdf) files
Data processing	Files read into MATLAB using netcdf read function. A 240 m vertical, 1800 sec time averaging filter used before plotting.
Coordinates	36.6060N -97.4850E
For more info	http://www.arm.gov/publications/tech_reports/handbooks/vceil_handbook.pdf
Raw data info	30 m vertical resolution & 15 sec between scans 11.5 sec integration time / Backscatter recorded in units of $(srad*km*10^4)^{-1}$ Files read into MATLAB using netcdf read function. A 240 m vertical, 1800 sec time averaging filter used before plotting.

MPL at SGP

Operational period	5/02/2006 to present
Data source	www.arm.gov
File type	sgpmplpolavgC1 files (e.g. sgpmplpolC1.b1.20080618.000001.cdf)
Data processing	Files read into MATLAB using netcdf read function (script name mpl_miport). Converted cdf variable #37 (signal_return_co_pol) to normalized backscatter by applying an overlap correction supplied by Rich Coulter (rlcoulter@anl.gov) and multiplying by the range squared (script mpl_range_overlap_correct). For final plotting, range overlap corrected data was loaded (using cos_summary_plot2 script), smoothed using a filter size of 90 sec in time and 150 m in space, and then plotted.
Coordinates	36.6060N -97.4850E
For more info	http://www.arm.gov/instruments/instrument.php?id=mpl&site=SGP
Wavelength	523 or 527 nm

WBI Continuous Gas Measurements. Figure 7 below shows the 3 tower levels, and the met instruments and gas inlets on a boom. Figure 8a shows the container that has meteorological instruments on the top, and gas instrumentation inside. Figure 8b shows the continuous gas samplers inside the trailer.
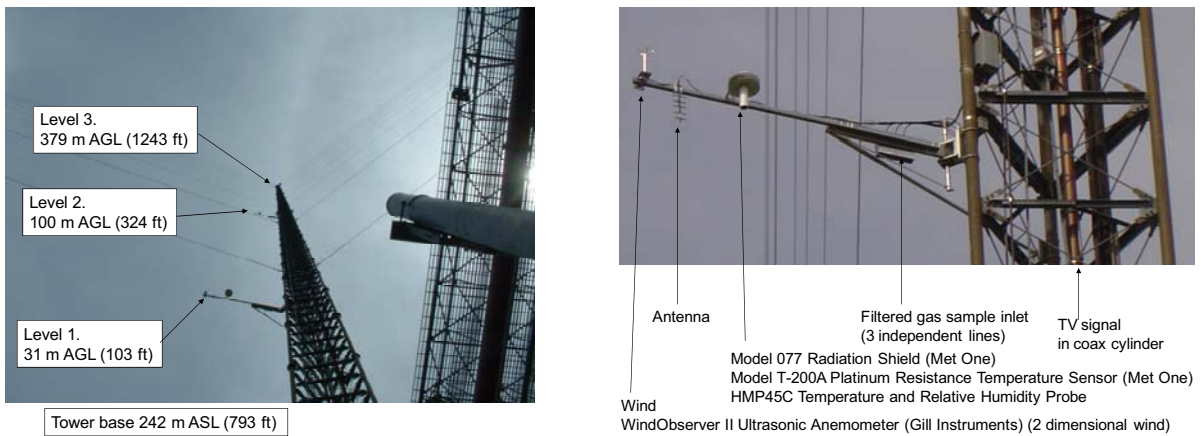

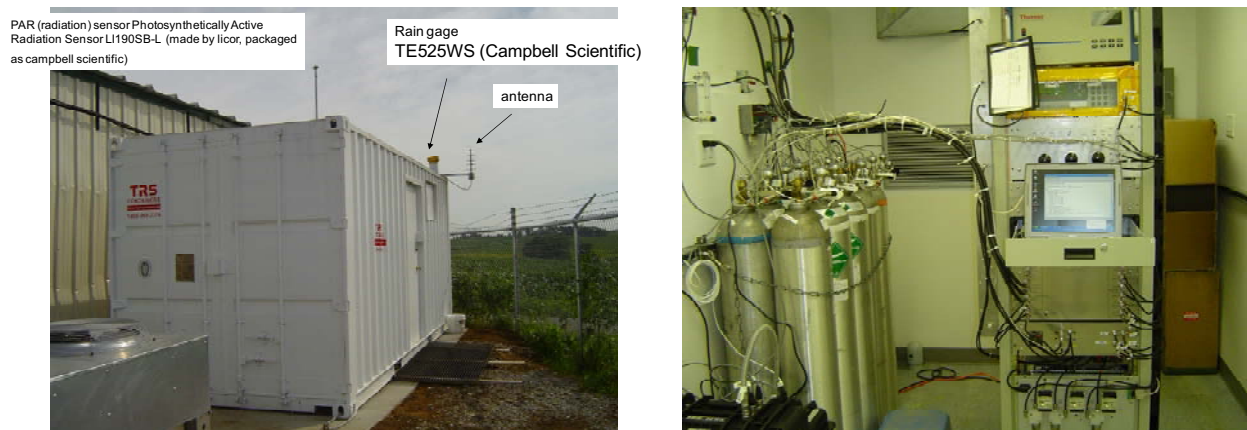Figure 7. Sampling / met booms on WBI tall tower

Figure 8. Enclosure and gas samplers at WBI.

WBI Sondes. Twice daily sondes were launched during summer 2008 at WBI by Liza Diaz of Ken Davis's group (Penn State). However, these launches were in June prior to the CL31 deployment. The main objective of the sonde launches was to allow temperature correction of NASA's DIAL CO2 LIDAR that operated at WBI during June 2008.
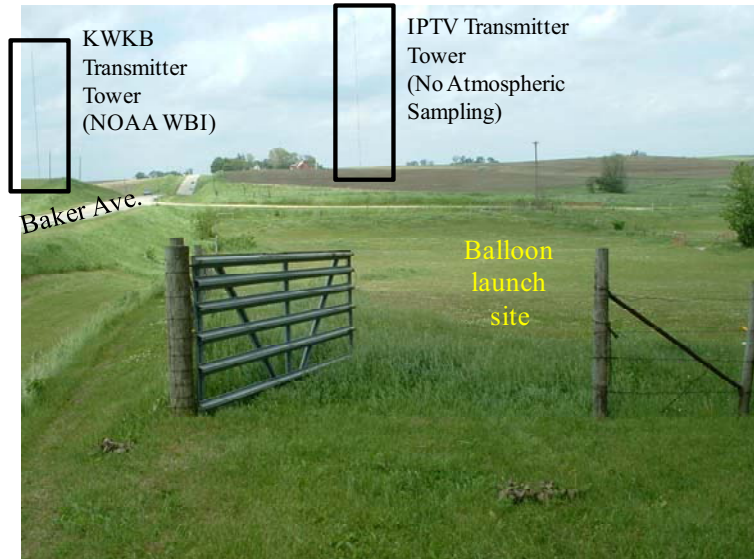

Figure 9. PSU rawinsonde launch location. View north from Bailey farm driveway.

2.3   Other Experimental and Data Analysis Aspects

Time Zones Both UTC and local times are used in this document. Both the SGP and WBI sites are in the Central Time Zone and experience daylight savings time correction during summer 2008. An example of the time conversion is as follows:

- 17:29:00 UTC = 12:29:00 CDT = 11:59:00 CST

Sunrise was at approximately 6 AM local time at SGP. For example, on June 18, SGP sunrise was at 06:09 CDT (11:09 UTC) while sunset was at 20:50 CDT (01:50 UTC).

Analysis of Planetary Boundary Layer features in the SGP Rawinsonde Data
The rawinsonde reports the dry bulb and dew point temperatures and potential temperature had to be calculated as follows:

$$T_{Potential} = T_{Dry} \left(\frac{1000}{P}\right)^{.286}$$

where P is the atmospheric pressure hPa, and $T_{Potential}$ and T_{dry} are both in Kelvin. Layers within the atmosphere can be determined by inversions in the potential temperature graph. When the potential temperature graph is vertical, there is a neutral layer in the atmosphere, and when the graph suddenly deviates from vertical, there is a transition from one layer to another.

The PBL features in the sonde data are listed in Appendix A. The classification scheme used is discussed here.

Kovalev and Eichinger (2004) review definitions of the planetary boundary layer. They list 8 definitions based on profiles of turbulent variables which are not used in this work (e.g. fluxes, variances, TKE, etc.). They also list 8 definitions based on profiles (page 491):

Convective Boundary Layer
  1. Height of a zone with significant wind shear
  2. Base of an elevated inversion or stable layer
  3. Height at which a rising parcel of air becomes neutrally buoyant during the day
  4. Height at which moisture or aerosol concentration sharply decreases
  5. Height at which single plume vertical velocities vanish
Stable Boundary Layer
  6. Height of the first discontinuity in the temperature, humidity, aerosol, or trace gas concentration profiles
  7. Upper boundary of a layer of significant wind shear
  8. Top of the surface inversion or stable layer
  9. Height of the low-level jet

In this work, only temperature and water vapor profiles were used, so the PBL heights determined from the rawinsonde data correspond to definitions 2 & 3 (using potential temperature), 4 (using water vapor profile), 6 (using temperature and water vapor), and 8 (using potential temperature). Appendix A classifies the rawinsonde features into 6 qualitative classes.

University of Iowa Sonde Feature Class	Corresponding PBL Definition from Kovalev and Eichinger
I -- Stable or very stable nocturnal BL (~5° per 100m) capped by a slightly stable or neutral layer.	8
II – Potential temperature inflection from stable to slightly stable or neutral	8
III – 100 m thick "kink" in potential temperature, separating ~neutral layers above and below by a more stable layer. Often drop in dewpoint with increasing elevation over the kink.	2 or 6
IV – Same as type II, except the layers in question are clearly stable (although not strongly stable).	2 or 6
V – In slightly stable or neutral layer, almost no signal in potential temperature, but sharp increase in dew point	6
VI – shift from unstable to neutral	3

The Iowa boundary layer detection algorithm was implemented in MATLAB and operates as follows. An averaged backscatter profile (y-axis) for one time is plotted against the height (x-axis). A fifth order polynomial (p) is fitted to the $\log_{10}$ of the backscatter profile. The second derivative (d^2p/dx^2) is found in order to find the inflection points ($d^2p/dx^2 = 0$) of the polynomial (p). The slope of each inflection point is determined and the inflection point with the steepest downward (most negative) slope is defined as the boundary layer height. The reason for this is the boundary layer is where the aerosol concentration greatly decreases, marking the transition from a well mixed to an unmixed layer of the atmosphere.

Section 3. Instrument Intercomparison at SGP

3.1 Weather Overview

Because of the high volume (~20 balloon releases per week at SGP) of data to be analyzed, we focused on a single week for intercomparison. This is the week of beginning Wednesday, June 18. Please note that winds analyzed here are from a mesoscale model (see Appendix F), rather than from site data.

- Wed June 18 – Surface temperatures from 20-30°C. Synoptic winds from east and southeast. Clouds and precipitation off and on. Clearing in early afternoon (local time).
- Thur June 19 – similar to 18th, except clouds all day between 1 and 2 km (per ceilometers), rain during the daylight hours (per EDAS).   Moderate synoptic winds from east and south.
- Fri June 20 – surface pressure increases steadily. Clouds clear in the AM. Winds from North.
- Sat June 21 – No clouds seen by ceilometer until PM. EDAS shows wind shift at around 7 AM local time. Initial strong (from) NE wind transitions to light wind from west. Strong AM stable layer, presumably from cloud free radiative surface cooling, and then ABL reaches 2.5 km in late afternoon, probably with cumulus cloud layer at 2.5 km. EDAS cloud cover not agree well with ceilometer, but this could be high cloud vs. total clouds – or just model resolution / error.
- Sun June 22 – No major clouds, no precipitation, calm NE winds rotate around during night to S-SW winds during daytime. Temp starts at 18 C and reaches 32 C at surface. Strong nocturnal inversion, and then strong development of high mixed layer.
- Mon June 23 – Steady synoptic winds from south, but no precipitation.   AM surface temp ~20 C, reaching > 35C in afternoon. Mixed cloud cover indicated by EDAS.
- Tues June 24 – Very similar to 23rd. Moderate winds from south continue and mixed cloud c

EDAS meteograms and the UNISIS surface weather composites can be found in Appendix F.

3.2 Analysis of Rawinsonde Data

Appendix C has relative humidity and potential temperature vertical profiles for each rawinsonde launch between June 18 and June 24. The actual figures that were analyzed to determine boundary layer features included these variables, and the water vapor mixing ratio and temperature. The results are summarized in table 3. A list of features can be found in appendix A.

Table 3. Chronological summary of key boundary layer features seen by sondes.

	00:30 CDT	6 AM	Noon	18:00
June 18	Stable NBL ~ 100m. Temperature inversions at ~1.1 and 3.5 km. Cloud layer (RH >90%) reaching to 3.5 km Cold, dry layers beginning at 5 & 7 km. Layer beginning at 7 km is dry and stable (FT?)	No sounding.	Unstable BL (100 m) capped by neutral mixed layer to 800 m. Temperature inversions at 0.8 and 2.3 km. FT (cold, dry, stable) seems to begin at ~4.5 km.	No sounding.
June 19	No sounding.	Stable NBL ~1.1 km thick. Capped by slightly stable/neutral layer and probable clouds at 3 km. Residual layer ht possibly set at 3 km. Multiple temperature inversions from 1-4 km. FT appears to start at 6.5 km.	Neutral BL, ht of 1 km. Capped by stable layers. One week temperature inversion at ~ 4 km. No clouds (based on max RH of 75%)	Shallow neutral BL of ~200 m, capped by multiple stable layers. High RH at 6-7 km.
June 20	Stable NBL ~100m. Overlaid by various stable (but less stable) layers, no clouds. Weak inversions at 1.1 and 2km.	Stable NBL ~350 m. Overlaid by various stable (but less stable) layers. No clouds, no inversions.	Unstable BL (100 m) capped by neutral ML to 1.6 km. 1.6 km is also top of cloud layer (judged by RH > 90%).	Neutral ML to 1.7 km. No cloud layer. Overlaid by various stable layers, no inversions, no clouds.
June 21	No sounding.	Strongly stable NBL to 100m. Capped by layers of various (lesser) stability, but no clouds and no temperature inversions.	No sounding.	Neutral ML to 2.5 km, possibly with cloud layer at 2.5 km. Capped by stable, cloud free conditions.
June 22	Very stable NBL of 200 m. Overlaid by various stable (but less stable) layers, no clouds. One small temperature inversion at 3.7 km.	Very stable NBL of 500 m. Overlaid by various stable (but less stable) layers, no clouds. No temp inversions.	BL grown to 2 km. Cloud free. Overlaid by stable layers. One small inversion at 4.5 km.	Stable BL ~ 100m thick, overlaid by neutral layer. Stability gradually shifting to stable, with the transition most pronounced at ~3 km. No clouds. No inversions
June 23	Stable NBL of 200m build up. Overlaid by various stable and neutral layer. Dewpoint drop and increased stability above 5 km.	Very stable 200m layer, and stable up to 1.1 km elevation. Overlaid by slightly stable layers, capped by cloud deck that seems to go from 4-5.5 km.	Temperature inversion at 400-500m, showing BL has grown to this elevation. Capped by continuous stable conditions, no inversions. Possible clouds at 4.5 km.	ML grown to 1.5 km. One small additional inversion at 2 km. Possibly still clouds at 4-5 km.
June 24	Stable NBL of 700m. Overlaid by various stable layers, but no inversions or clouds. Dewpoint feature at 3.5 km.	Stable NBL extending to 1.5 km. Stratified within that 1.5 km thickness. Small inversions at 4 and 5 km. No clouds likely.	Unstable BL of 100m. ML depth 2 km. No clouds likely. One small inversion at 5 km.	Neutral to slightly stable at 1 km. Slightly stable to stable at 4 km. Cloud deck likely between 5 and 6.5 km, and possibly from 4-5 km. Small inversions at 4 and 6.5 km.

3.3 SGP Intercomparisons

Validation of ceilometers data processing A CL31 24 hour curtain plot is shown in figure 10. The left plot was generated at Vaisala, while the right plot was generated with the same averaging time at the University of Iowa. One different in the plots is that the Iowa spatial averaging was done on a straight vertical basis, while the Vaisala spatial averaging was done on a 3° tilt. The similarities in the qualitative picture were an important check of new data processing scripts written at Iowa.
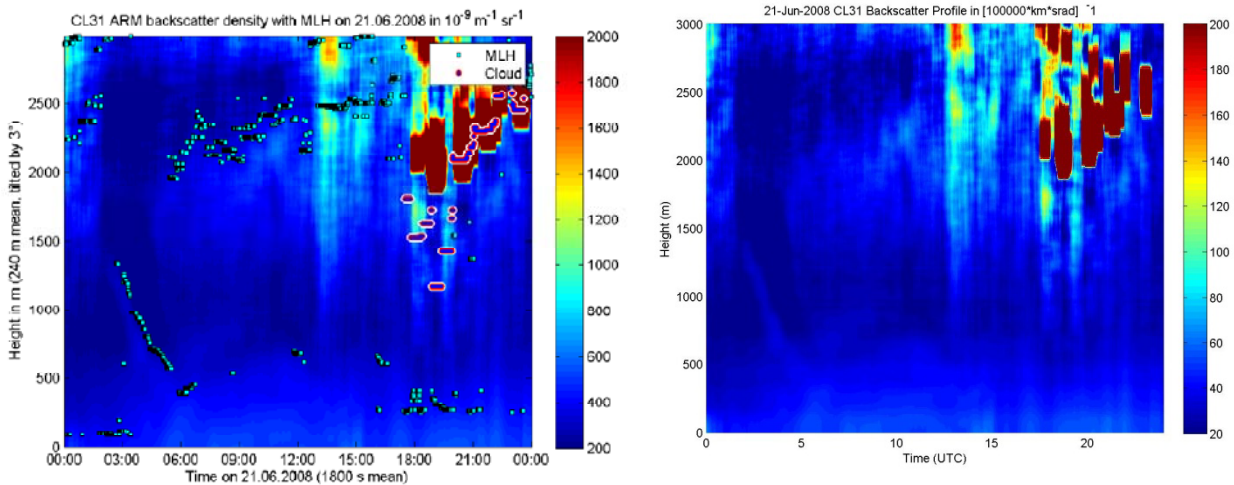
Figure 10. 24 hour curtain plot of SGP backscatter measured by CL31 and processed by Vaisala (left) and processed by U Iowa (right). Difference in axis (2000 vs. 200 maximum scale) is consistent with difference in units.

CL31 compared with CT25. A sample plot of both instruments plotted side by side for the same day is shown below. All plots have been filtered to reduce or eliminate noise in the return signal detected by the ceilometers (filter settings found in Table 2). Many more intercomparisons, including vertical profiles of backscatter, can be found in Appendix C. Conclusions drawn from the appendix C plots include:
- Overall, the qualitative return from both instruments was very similar (e.g. June 19th 17:29Z; 20th 05:43Z, 20th 17:30Z).
- The spatial and temporal resolution of the CL31 was superior to that of the CT25K.
- The signal to noise ratio appears to stay stronger to higher altitudes with the CL31 (e.g. 20th 05:43Z about 1500m).
- At altitudes less than 100 m, the CT25K and CL31 are qualitatively different, with the CT25K usually having a backscatter peak highest at around 80 m, and the CL31 product smoothly increasing up to the a maximum at the surface (e.g. 20th 05:43Z; 22nd 05:29Z).
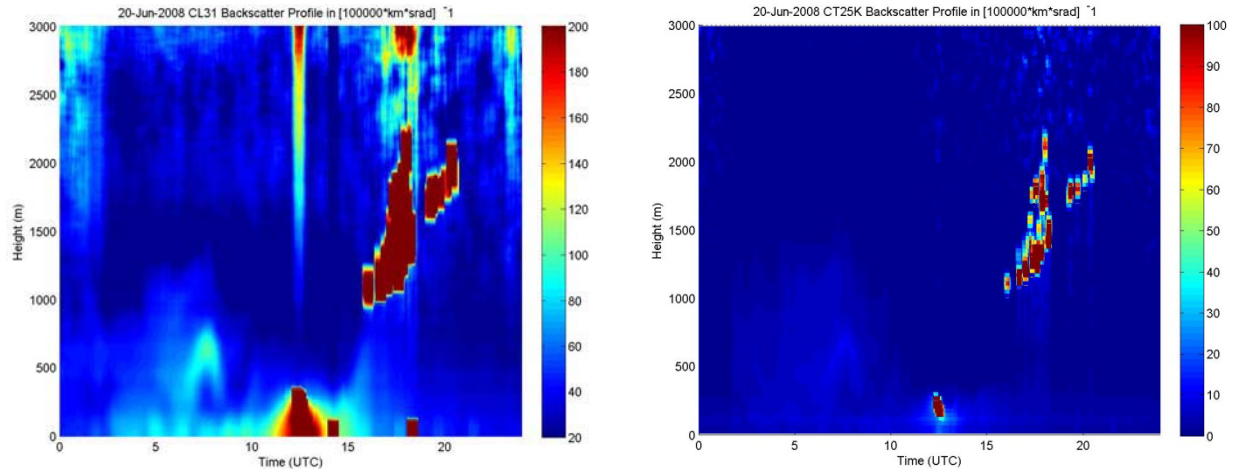
Figure 11. CL31 (left) and CT25K (right) backscatter profiles for June 20, 2008.

Boundary layer height as viewed by sondes vs. CL31, and CL31 vs. MPL.   The rawinsonde can give the most precise data for the BLH at one point in time and in space. Comparison between the sondes and the CL31 is the primary method of comparison that we are using in evaluating the instrument.   An example of the comparison is shown in the figure below, and similarly constructed figures for each balloon release from June 18 – June 24 can be found in appendix C.

Figure 12 combines in one figure all of the visualization/analysis techniques employed for SGP. The sondes and the remote sounding vertical profiles are all shown together. The manually identified "boundary layer features" (listed in Appendix A) from examination of the sonde vertical profiles are shown with the vertical profiles and with the backscatter curtain plots. MLH and CLH identified by automated software are also shown.

In this particular figure, the sonde was launched at close to midnight local time, through a stable PBL with three sublayers. The first sublayer is the most stable layer and has the highest relative humidity and aerosol concentration, and goes from the surface to about 100 meters. From 100 meters to around 1000 meters is a slightly stable layer capped by a sharp increase in potential temperature and drop in relative humidity. This layer is cut in two at 500 m by a thin layer of slightly increased stability and lower RH. The heights of these features (100 m, 500 m, 1000 m) are marked as horizontal lines in all the panels of the plot. Qualitatively, all of ceilometers/lidar plots are similar. The algorithm retrieved boundary layer heights are shown in the CL31 (second plot). The red/white squares are from the Vaisala algorithm, and seem to coincide with the kink in the CL31 backscatter profile at about 200 m. The green/black circles are from the Iowa algorithm, which is based on the elevation where the $\log_{10}$(backscatter) decreases fastest, and this occurs between 300 and 500 m. At the time of this sonde, there is no strong feature in the backscatter profile corresponding to the kink in the potential temperature at 100 m. However, soon after 5:40 UTC, the CL31 algorithm does begin to identify a boundary layer at 100 m.
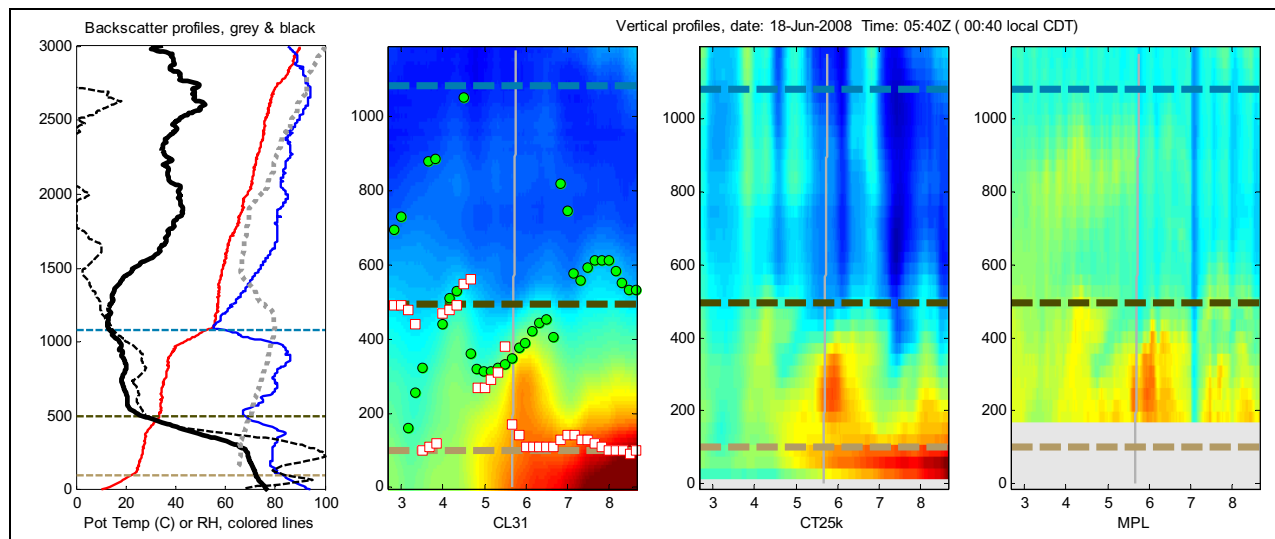
Figure 12. Comparison of vertical profiles as seen by weather balloon, CL31, and MPL at 05:40 UTC on June 18.

Left panel The red and blue lines show rawinsonde data. Relative humidity (blue line) from the sonde, and it corresponds to the 0-100 scale at the bottom of the plot. Potential temperature (red line) is NOT TO SCALE; it has been normalized to increase dynamic range. Black and grey vertical profiles are backscatter profiles from the CL31 (thick solid line), the CT25K (thin dashed black profile), and MPL (grey dotted profile).

Horizontal lines are heights of features in potential temperature or RH from sonde

Following to the right are curtain plots showing backscatter (color) versus height (y axis, meters) and time (x axis, UTC hours) for the CL31, CT25k, and MPL. These are centered in time on a balloon launch. The balloon elevation vs. time trajectory is shown by the grey vertical line at the center of each curtain plot. Color scales have been adjusted to maximize contrast of concentration gradients and are not comparable from day-to-day or instrument-to-instrument.

Green dots are MLH calculated by Iowa algorithm. White/red squares are MLH calculated by Vaisala algorithm. Blue/red circles are cloud layer height by Vaisala algorithm

NOTE: height scale changes between the lefthand plot and the curtain

Similar plots for additional week 1 balloon launches can be found in appendix C.

For an example of an afternoon sonde that encounters a growing unstable boundary layer, see appendix C. For example, June 20 at 17:30 UTC has a growing mixed layer with clouds, and June 23 at 17:48 UTC has a growing mixed layer without clouds.

The boundary layer heights determined by the algorithms and the boundary layer features from examination of the sondes are compared as time series and as a scatterplot in the following figures.
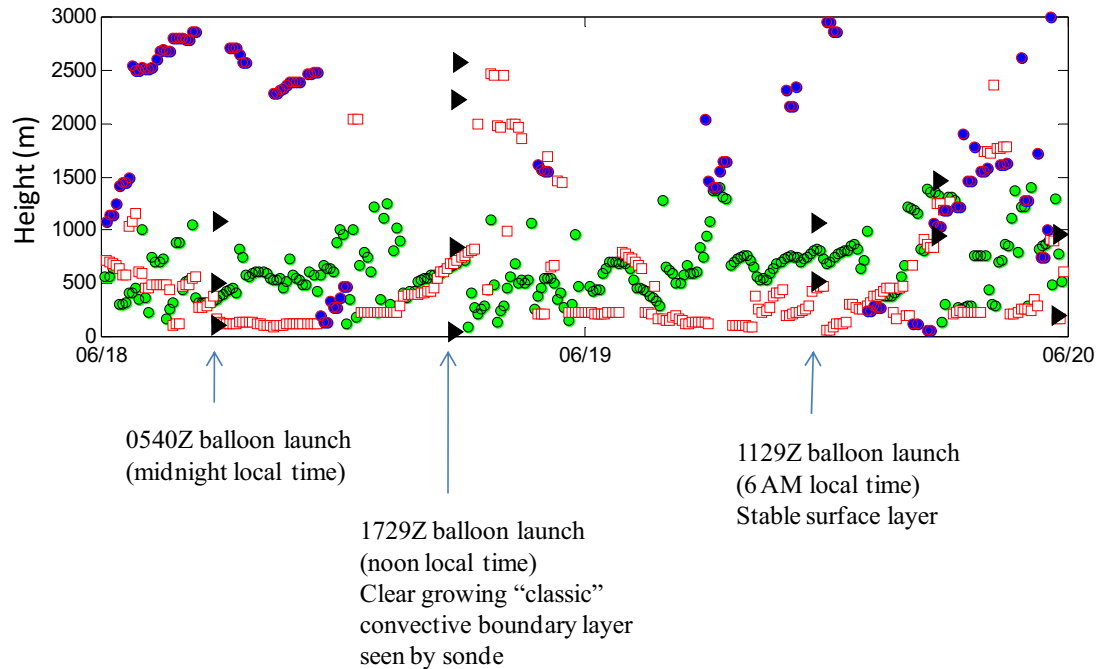
Figure 13. Two day time series of boundary layer features. Date tick marks are at 00:00 UTC, which is 18:00 central standard time. Both daytime periods have growing boundary layers that are (a) recovered by both algorithms, and (b) have close matches between the sondes and the ceilometer-derived heights. On the 19th, the rising BL forms a cloud deck at beginning at noon (standard time) at around 1000 m. This BL growth and cloud detection can be seen in Appendix C, June 19 17:29 UTC plot.

The boundary layer algorithms were applied in a manner which recovers a single MLH. Both algorithms could be applied to extract multiple mixed layer heights. A more sophisticated application of these algorithms would be needed to extract a single height that corresponded to either the maximum height of a nocturnal stable layer, or the maximum height of a daytime mixed layer.

The Iowa algorithm was run to select the most prominent decay in the $\log_{10}$(backscatter) in the elevation range between 100 and 3000 m. This fails when the feature of interest is at low altitude or when the feature is at high concentration (using the log of backscatter emphasizes lower concentrations). It also fails when clouds are present, since this makes a backscatter feature that cannot be fit easily by a 5th order polynomial.

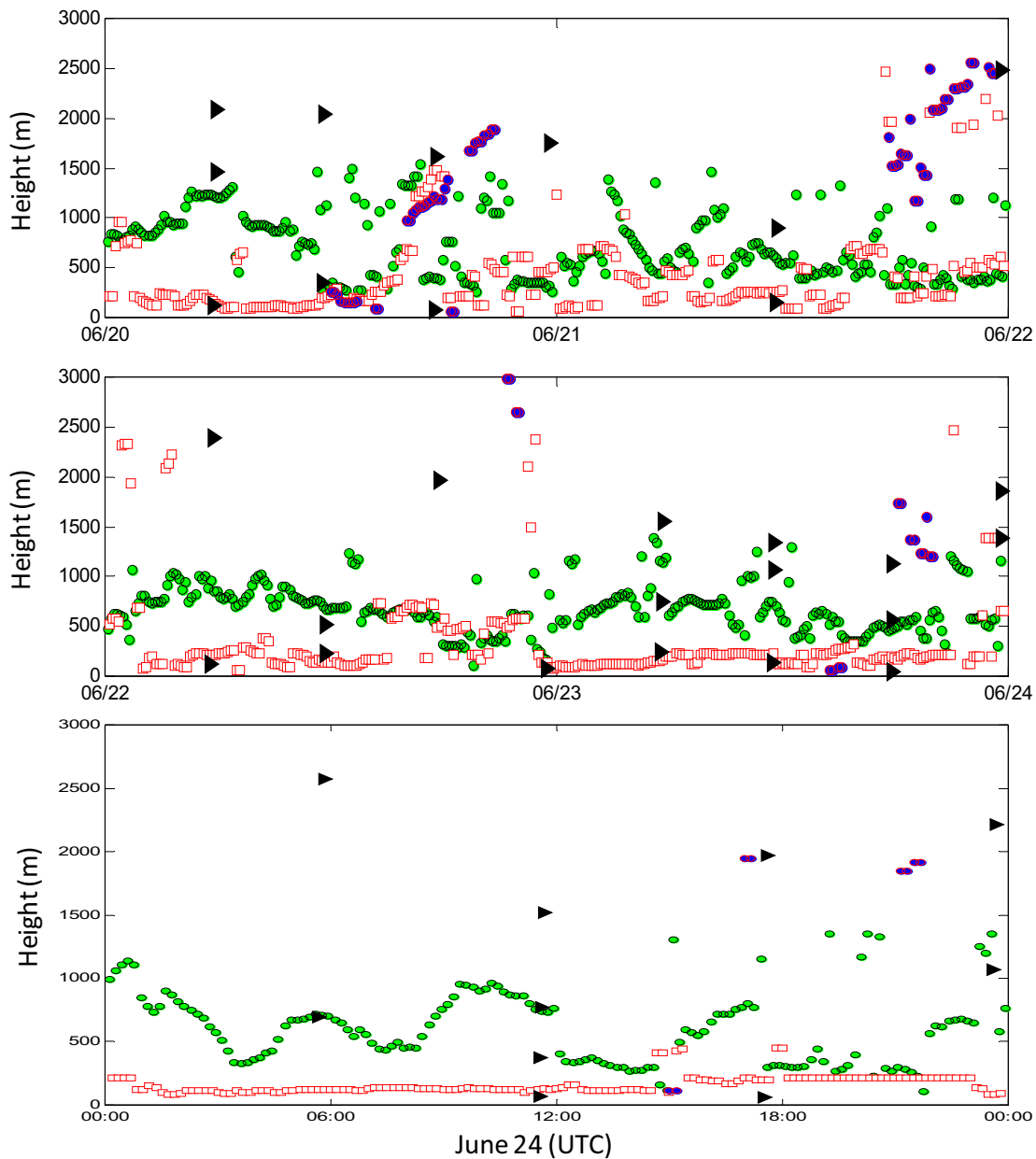The Vaisala algorithm can be run to detect multiple boundary layer heights.

Figure 14. 5 days of comparison of algorithm- and sonde-derived boundary layer heights. Panel A covers June 20 and 21 (strong nocturnal inversion layers). Panel B covers June 22 and 23, which are mostly cloud free and have mixed layers that grow, but not to very high altitudes. Panel C shows June 24. See appendix C for the June 24 17:29 UTC sonde, where the algorithms (as implemented in this work) miss the growing boundary layer.

What is striking in figures 13 and 14 is how many sonde-derived boundary layer features <u>do</u> have a corresponding CL31-derived boundary layer height (from at least one of the algorithms). Plotting the CL31-derived heights versus the nearest sonde-derived height gives figure 15. Figure 15 shows that many of the CL31-derived heights have a corresponding sonde-derived

height within about 15%. The Iowa algorithm (green dots) was more likely to recover features at higher altitude, and the Vaisala algorithm (black squares) was more likely to get lower altitude features. Below 500 m, the Vaisala algorithm tended to cluster the height around a smaller range (120-220 m) than determined by the sondes (40-350 m). Therefore, relative error in the boundary layer height is high.
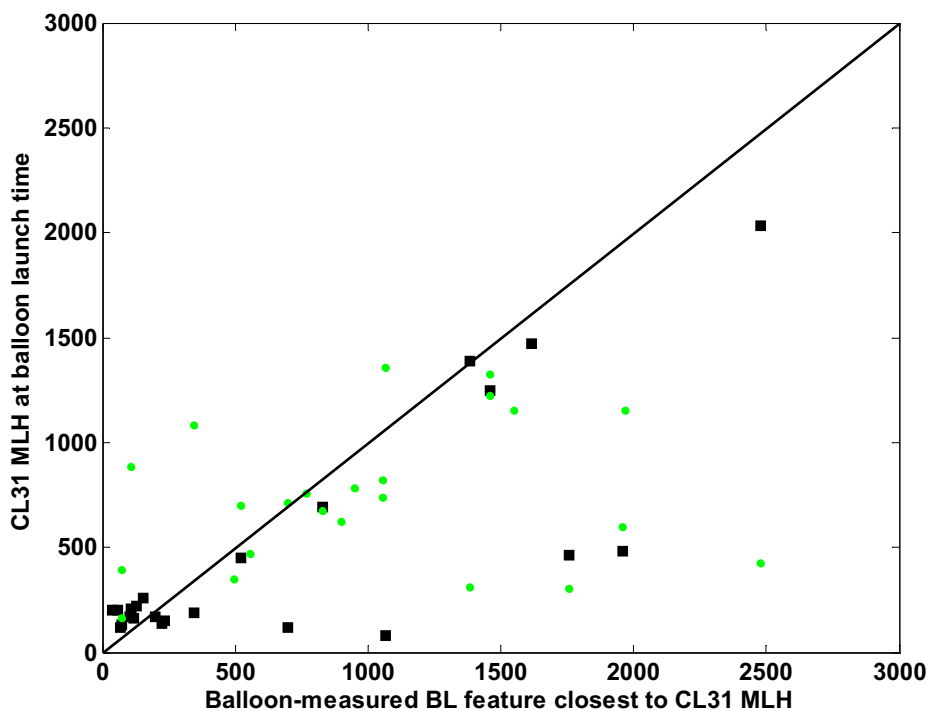

Figure 15. Overall comparison of boundary layer heights from rawinsonde versus algorithms fed with CL31 data. Vaisala algorithm (black squares) and Iowa algorithm (green dots).

Section 4. CL31 at WBI

At WBI, the intercomparison is between the CO_2 time series measured at different tower elevations, and the CL31 curtain plot and boundary layer heights. Figure 16 shows one day of data from the CO_2 and CL31 instruments.
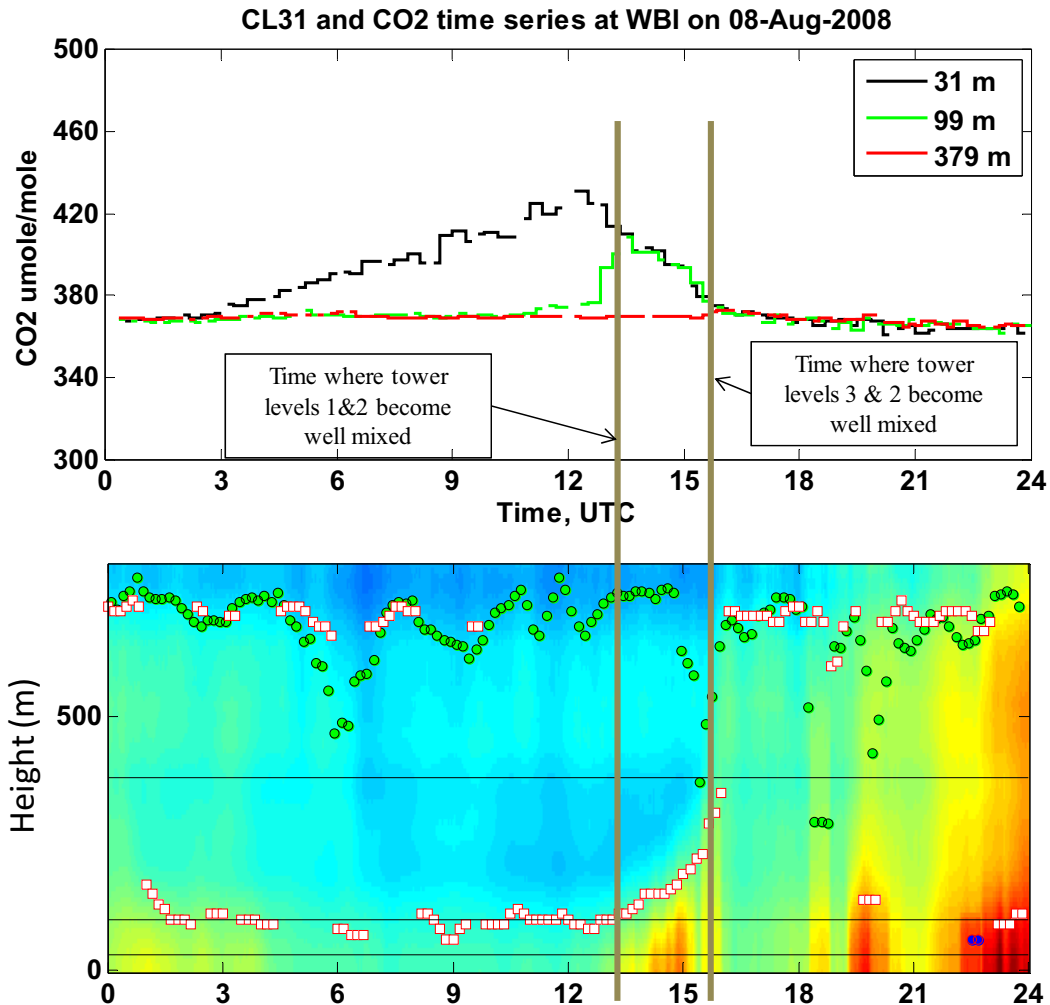
Figure 16. CO_2 and Ceilometer time series for August 8, 2008 at WBI. Software retrieved boundary layer heights are shown from the Iowa algorithm (green/black circle) and the Vaisala algorithm (red/white squares). Brown vertical lines show the time when the mixed layer gets to 99 m and 379 m, as determined by the convergence of the CO_2 concentrations.

Appendix E has the corresponding plots for other days. From the appendix E plots, we conclude the following:

- The ceilometer-derived boundary layer height and the time where the level 1 (31 m) and level 2 (99 m) CO2 concentrations converge is not correlated. The reason for this is that the Vaisala BL height stays around 100 m all night. In only one of 6 cases examined (Jul 28), the Vaisala-derived boundary layer height could predict the time of level 1 & 2 mixing.
  - However, in three of the 5 remaining cases, there were features in the CL31 time series that could did correlate with the time of mixing to 100 m. In two cases

(Aug 6 and Aug 8), backscatter increases sharply in the 0-100 height range at the time when the CO2 values converged. In one case, the backscatter decreased sharply.

- The ceilometer-derived boundary layer height and the time where the level 2 (99 m) and level 3 (379 m) CO2 concentrations converge is correlated, at least on some days. In the 6 days subjected to detailed examination, during one day levels 2 and 3 did not correlate at all, and this was consistent with a low mixed layer height (that did not reach tower level 3; Aug 6). In the remaining 5 cases, there were features in the CL31 at the time of CO2 convergence (either surface aerosol concentration increases or decreases consistent with convective mixing). In 3 of the 5 cases, the software-derived boundary layer height routines identified the mixed layer as crossing 389 meters at the same time as the CO2 convergence.

5. Conclusion

The value in the CL31 measurement coupled with the tower-based CO2 measurement is not to tell something we already know (the time the mixed layer reaches 379 m), but rather to quantify how high the mixed layer grows during the afternoon.

Additional literature review and modeling (e.g. synthetic data experiments with known fluxes, and either correct or systematic errors in boundary layer heights) would be needed to determine what leverage increased knowledge of local boundary layer height and structure would have on the top-down inverse problem. However, from a measurement standpoint, it does seem feasible to constrain both nocturnal and daytime boundary layer heights, and their temporal patterns at individual sites using ceilometers. This constraint is limited by the potentially complex nature of the planetary boundary layer, and by the differences in ideal measurement (e.g. potential temperature, water vapor and turbulent fluxes) versus the actual remote measurement (backscatter).

Substantial work would be needed, probably on a site-by-site basis and involving intensives with rawinsonde releases during multiple seasons, to validate the boundary layer measurement and to fine tune the software so that the appropriate boundary layer features were being extracted. This will be especially during periods with multiple layers.

References

Kovalev, V., and Eichinger, W. (2004) Elastic Lidar: Theory, Practice, and Analysis Methods. Wiley Interscience. Hoboken, NJ.

Appendices

A Boundary layer height analysis of rawinsondes (week of June 18)

B Curtain plots from CL31 (SGP and WBI) and CT25k (SGP)

C Rawinsonde – CL31 – CT25k – MPL Comparisons

D ARM-SGP Data Analysis by Vaisala, Reijo Roininen

E Daily time series of CO2 and CL31 for selected days, WBI

F Raw rawinsonde plots, EDAS weather information, and surface weather maps (week of June 18)